Semaphorin 6A regulates angiogenesis by modulating VEGF signaling

*Marta Segarra,[1] *Hidetaka Ohnuki,[1] Dragan Maric,[2] Ombretta Salvucci,[1] Xu Hou,[3] Anil Kumar,[3] Xuri Li,[3] and Giovanna Tosato[1]

[1]Laboratory of Cellular Oncology, Center for Cancer Research, National Cancer Institute, National Institutes of Health (NIH), Bethesda MD; [2]Laboratory of Neurophysiology, National Institutes of Neurological Disorders and Stroke, NIH, Bethesda MD; and [3]National Eye Institute, NIH, Rockville, MD

Formation of new vessels during development and in the mature mammal generally proceeds through angiogenesis. Although a variety of molecules and signaling pathways are known to underlie endothelial cell sprouting and remodeling during angiogenesis, many aspects of this complex process remain unexplained. Here we show that the transmembrane semaphorin6A (Sema6A) is expressed in endothelial cells, and regulates endothelial cell survival and growth by modulating the expression and signaling of VEGFR2, which is known to maintain endothelial cell viability by autocrine VEGFR signaling. The silencing of Sema6A in primary endothelial cells promotes cell death that is not rescued by exogenous VEGF-A or FGF2, attributable to the loss of prosurvival signaling from endogenous VEGF. Analyses of mouse tissues demonstrate that Sema6A is expressed in angiogenic and remodeling vessels. Mice with null mutations of Sema6A exhibit significant defects in hyaloid vessels complexity associated with increased endothelial cell death, and in retinal vessels development that is abnormally reduced. Adult Sema6A-null mice exhibit reduced tumor, matrigel, and choroidal angiogenesis compared with controls. Sema6A plays important roles in development of the nervous system. Here we show that it also regulates vascular development and adult angiogenesis. (*Blood*. 2012;120(19):4104-4115)

Introduction

Angiogenesis during development and in adult mammals proceeds largely through endothelial cell sprouting and sprouts remodeling to generate a network of vessels where blood can flow. VEGF-A, its receptor VEGFR2, and coreceptor neuropilin-1, Notch ligands, and Notch receptors, B-ephrin ligands, and EphB receptors, and other molecules are critical mediators of angiogenesis, but aspects of this process are not explained and other molecules probably contribute.

The semaphorins comprise a family of membrane-bound and secreted proteins implicated in the development of the neural system, and in modulating immune responses and tumor growth in the adult.[1-3] Semaphorins are characterized by the presence of a Sema domain, a 500 residue N-terminal domain, structurally similar to the extracellular domain of α-integrins, and a determinant of receptor binding specificity.[4] There are 8 classes of semaphorins, including classes 1 and 2 found mostly in invertebrates, classes 3 to 7 found in vertebrates, and the viral (V) class encoded by viruses. Semaphorins signal through their plexin receptors, but whereas membrane-bound semaphorins bind directly to their cognate plexin receptors, the secreted class-3 semaphorins require neuropilin-1 or 2 as coreceptors.[5,6] Plexin receptors can elicit multiple signaling pathways in response to semaphorin activation, as they associate with various signaling protein partners.[6]

Many secreted class-3 semaphorins have been reported to inhibit angiogenesis.[2] Semaphorin-3A (Sema-3A), which binds neuropilin-1 and signals through plexinA1, A2, or A4, inhibits endothelial cell responses to $VEGF_{165}$ in vitro.[7-12] However, it is not clear whether Sema3A is required for normal vascular development. Whereas early studies described a vascular phenotype in Sema3A-null mice,[9] other studies reported no defects in the formation of the major axial vessels, vessel branching or remodeling in these mice.[13] No overt vascular defects were observed in mice expressing a mutant neuropilin-1 that impairs semaphorin signaling,[14] or in mice lacking expression of plexinA2, A3, and A4.[13]

Emerging observations suggest a vascular role for class-6 Semaphorins, which comprise the 4 transmembrane proteins Sema6A-Sema6D. Plexin-A2 and plexin-A4 are the receptors for Sema6A and 6B, whereas plexinA1 is a receptor for Sema6C and Sema6D.[15-18] The recombinant ectodomain of Sema6A-1, a variant semaphorin closely related to Sema6A, was reported to inhibit endothelial cell growth and experimental tumor angiogenesis, but the mechanism was not clear.[19,20] Sema6D was reported to stimulate VEGFR2 signaling, attributed to plexinA1 receptor activation and Sema6D-dependent activation of VEGFR2.[21] Recently, Sema6B was reported to promote endothelial cell growth and enhance FGF2-induced proliferation.[20]

Through functional and biochemical studies in primary endothelial cells and the characterization of Sema6A-null mice, we show that Sema6A is a critical mediator of endothelial cell survival and a selective regulator of VEGF/VEGFR2 signaling.

Methods

Animals

The Sema6A-deficient gene-trap mouse line[22-24] was from Dr Mitchell (Trinity College, Dublin, Ireland). The day of birth is designated as postnatal day 0 (P0). All animal protocols were approved by the NCI-Bethesda animal care and use committee.

Cells and reagents

HUVECs were propagated with endothelial cell growth supplement (ECGS; Sigma-Aldrich) through passage 6.[25] For detection of endogenously phosphorylated VEGFR2, HUVECs were cultured in endothelial basal growth medium-2 (EBM-2 with FGF2, IGF-1 and EGF from EGM-2 BulletKit; Lonza). The murine cell lines B16-F10 (B16) melanoma and Lewis Lung Carcinoma/1 (LLC/1) from ATCC were propagated in DMEM with 10% fetal bovine serum (FBS). Recombinant human VEGF-A, FGF2, Sema6A-Fc, and IgG1-Fc were from R&D Systems. Human VEGF-A neutralizing antibody (Avastin; Genentech) was from the National Institutes of Health pharmacy. Na_3VO_4 was from Sigma-Aldrich. Propidium iodide, Hoechst 33342 and DAPI were from Invitrogen. Sorafenib tosylate was from Selleck chemicals.

Sema6A, *VEGFR2*, *plexinA2*, *plexinA4*, and *VEGFA* silencing

Sema6A, *VEGFR2*, *plexinA2*, *plexinA4*, and *VEGFA* expression was silenced with third-generation lentiviral vectors ([Vsv-g]-pseudotype HIV-1–based; shRNA).[26] Control (pLKO.1 puro), Sema6A, VEGFR2, plexinA2, plexinA4, and VEGFA shRNA vectors were generated by cotransfection of 293T cells with 4 plasmids: a CMV packaging construct expressing the *gag* and *pol* genes, a Rous sarcoma virus construct expressing *rev*, and a CMV construct expressing the *VSV-g* envelope, and a self-inactivating transfer construct (Mission shRNA lentiviral plasmid; Sigma-Aldrich) containing the expression cassette (human U6 promoter) for the shRNA and a cassette (human phosphor glycerate kinase promoter) for the *Puromycin* resistance gene. Virus-containing supernatant (collected 48 hours after transfection) was used for infection (overnight incubation with 8 μg/mL polybrene); puromycin (EMD Biosciences; 0.5 μg/mL) was used for cell selection over 7 days starting 72 hours after infection. Five human Sema6A lentiviral shRNA constructs were tested; the most effective (TRCN0000061111 and 61112) were selected for use. Five human VEGFR2 lentiviral shRNA constructs were tested, and found to be equally effective. Four human plexinA2 and plexinA4 shRNA constructs were tested; the most effective (TRCN0000061499 plexinA2, and TRCN0000078683 plexinA4) were selected for use. Two human VEGFA shRNA constructs were tested (TRCN000003343 and 3345); the most effective (TRCN000003343) was selected for use.

RNA isolation and measurement

Total RNA extracted with TRIzol (Invitrogen) was reverse transcribed using high-capacity cDNA reverse transcription kit (Applied Biosystems). Human Sema6A, VEGFR2, FGFR1, VEGF-A, plexinA2, plexinA4, and GAPDH; murine Sema6A, plexinA2, plexinA4, and GAPDH mRNAs were measured by real-time PCR using assay-on-demand Taqman gene expression probes (Applied Biosystems), as described.[27]

Cell proliferation

HUVECs were seeded (25 000 cells/well; 24-well plates) in complete culture medium. Growth curves were generated from time-lapse images obtained every 8 hours over 96 hours incubation using IncuCyte (Essen Instruments).

Flow cytometry

Viable, apoptotic and necrotic cells were measured after incubation with Hoechst 33342 and propidium iodide (Invitrogen).[28,29] For VEGFR2, phospho-Erk1/2 and phospho-AKT detection, trypsin-detached HUVECs were fixed (2% paraformaldehyde; 10 minutes), permeabilized (cold 90% MeOH 30 minutes, 4°C), washed (PBS with 1% BSA), blocked (0.5% BSA in PBS with 1mM Na_3VO_4; 30 minutes) and immunostained with rabbit IgG anti–human VEGFR2 (recognizes the intracellular carboxy-terminal domain), rabbit mAb to phospho-Erk1/2 (Thr202/Tyr204), or rabbit mAb to phospho-AKT (Ser473; all from Cell Signaling Technology; 1:200 dilution; 1 hour, room temperature) followed by staining with PE-labeled F(ab′)2 donkey anti–rabbit IgG antibody (Jackson Immunoresearch Laboratories;

30 minutes, room temperature). DNA content was measured by DAPI staining (1 μg/mL) after cell fixation and permeabilization.[29]

Western blotting

Protein extracts (RIPA lysis buffer with protease inhibitor cocktail setIII (Calbiochem), 50mM NaF, and 1mM Na_3VO_4) were resolved in NuPAGE 4%-12% Bis-Tris Gel (Invitrogen) and dry-transferred with iBlot system (Invitrogen). Membranes were probed with: rabbit mAb to phosphorylated VEGFR2 (Tyr 1175 and Tyr 951; Cell Signaling Technology), rabbit IgG anti–human VEGFR2, rabbit mAb to phosphorylated Erk1/2 (Thr202/Tyr204), rabbit mAb to total Erk1/2 (p44/p42), rabbit mAb to phosphorylated AKT (Ser473) IgG rabbit antibody to total AKT, rabbit mAb to cleaved Caspase 3 (all Cell Signaling Technology); goat antiactin (Santa Cruz Biotechnology) and rabbit anti–Neuropilin-1 (Invitrogen). Horseradish peroxidase (HRP)–conjugated rabbit anti–goat IgG-Fc was from Calbiochem; and HRP-conjugated donkey anti–rabbit IgG were from Amersham Pharmacia Biotech. Bound secondary antibodies were visualized by Immobilon Western chemiluminescent HRP substrate (Millipore); chemiluminescent signal was captured with ImageQuant LAS4000 technology (GE Healthcare).

Laser-induced choroidal neovascularization, matrigel, and tumor neovascularization

Laser-induced choroidal neovascularization (CNV) was performed as described.[30,31] Mice (6 weeks old) received 4 photocoagulation spots (75 mm size, 75 ms, 90 mW power)/eye at approximately equal distance from the optic nerve (Oculight infrared laser system; 810 nm; IRIDEX). Ophthalmic ointment was applied after laser treatment. After 7 days, eyes were removed and processed for immunostaining. Matrigel-supported neovascularization was evaluated as described.[25] Mice (5 weeks old) were injected subcutaneously with 0.5 mL matrigel (BD Bioscience) containing VEGF-A, FGF2 (150 ng/mL each; R&D Systems), and heparin sodium (0.5 mg/mL; Sigma-Aldrich). After 7 days, matrigel plugs were processed for histology, as described.[25] Tumors were induced (6- to 7-week-old mice) by subcutaneous abdominal injection of syngeneic B16 melanoma or LLC/1 carcinoma cell lines (10 × 10^{6}/mouse), as described.[27] After 10 (B16) or 12 (LLC/1) days, tumors were removed, weighed, and processed for histology.

Immunofluorescence microscopy and image quantification

HUVECs were grown on gelatin-coated glass chamber slides (Lab-Tech), fixed in 4% paraformaldehyde, immunostained with rabbit mAb to cleaved Caspase 3 (1:100; Cell Signaling Technology) followed by Alexa Fluor–conjugated 488 anti–rabbit (1:400 Invitrogen) and mounted (Vectashield containing DAPI; Vector Laboratories). Mouse eyeballs were fixed in 4% paraformaldehyde for 4 hours at 4°C. After removal of the sclera, the retinal cup (with hyaloid vessels and crystal body) was incubated (1 hour, room temperature) in PBS containing 1% Triton x100, 10% FBS, and 10mM glycine, and stained (1 hour, room temperature) with goat anti–mouse Sema6A antibody (1:50; R&D Systems) and rabbit monoclonal anticleaved caspase 3 (1:500; Cell Signaling Technology). Alexa Fluor 488–conjugated anti–goat IgG (1:2000; Invitrogen) and Alexa Fluor 594–conjugated anti–rabbit (1:2000 Invitrogen) were used for detection (30 minutes room temperature). The stained retinal cup was fixed (4% paraformaldehyde, 20 minutes room temperature), soaked (37°C, 18 hours) in 2% low melting temperature (LMP) agar in DPBS, and incubated for 3 hours, 4°C. The crystal body and retinal layer were removed. The LMP-agar embedded hyaloid vessels were flat-mounted with Vectashield containing DAPI (Vector Laboratories). Hyaloid vessel images were from a Zeiss LSM710 confocal microscope (Carl Zeiss) with 10× and 100× objective lenses using ZEN software (Carl Zeiss). The number of hyaloid vessel branches was quantified using OpenLab software (PerkinElmer).

The retina was incubated (15 minutes, 99°C) in TE buffer (pH 8.0), immediately cooled on ice, and further incubated (1 hour room temperature) in TBS containing 0.1% Tween 20 and 5% FBS. After blocking (Fc receptor blocker, 1 hour, room temperature; Innovex Bioscience), the
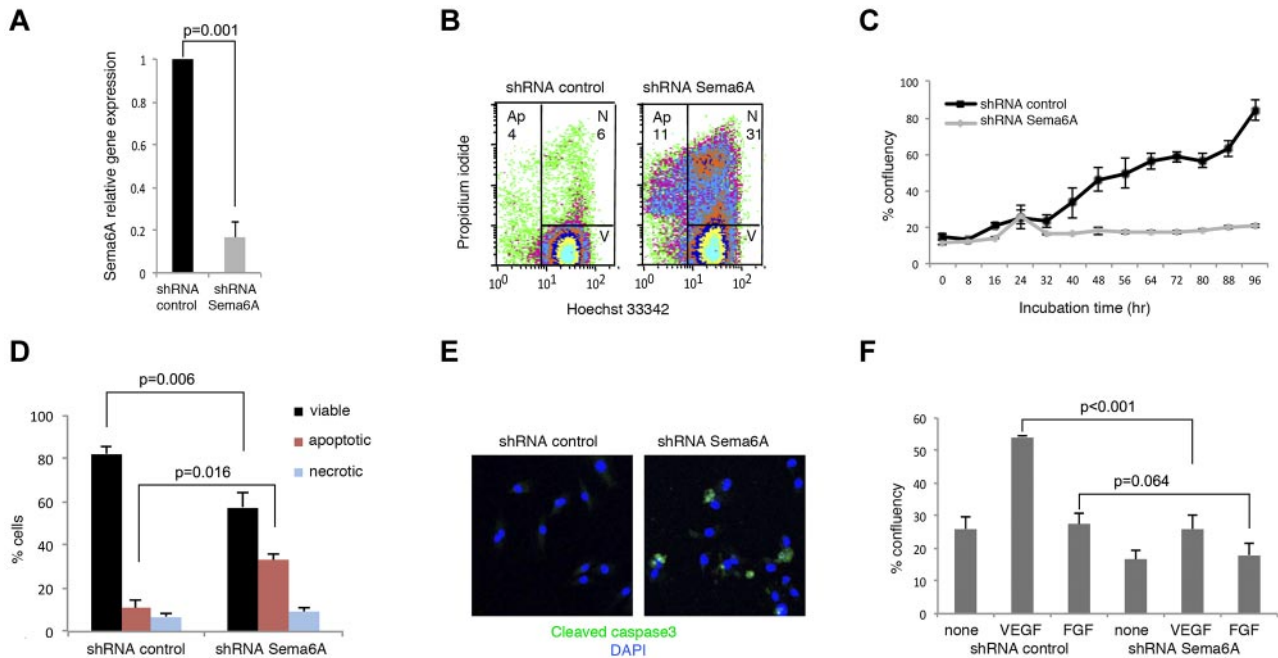
Figure 1. Silencing _Sema6A_ expression promotes endothelial cell death. (A) HUVECs were infected with lentivirus control (shRNA control) or _Sema6A_-silencing lentivirus (shRNA Sema6A); Sema6A expression was measured by quantitative PCR after 7-day puromycin selection. The results reflect the means ($\pm$ SD) of 4 experiments. (B) Seventy-two hours after infection, cells were stained with propidium iodide and _Hoechst 33342,_ and the distribution of viable (V), necrotic (N), and apoptotic (Ap) cells was measured by flow cytometry. (C) Growth kinetics of HUVEC measured by IncuCyte monitoring over 96 hours culture, beginning 72 hours postinfection with control or Sema6A shRNA. The results are expressed as mean ($\pm$ SEM, 4 replicate wells) percentage culture confluence/time point. (D) Cell death was measured by flow cytometry in _Sema6A_-silenced and control HUVEC (after lentivirus infection and 7-day puromycin selection). Results are from 4 independent experiments ($\pm$ SEM). (E) Cleaved caspase3 in _Sema6A_-silenced and control HUVEC detected by immunofluorescence staining. (F) _Sema6A_-silenced and control HUVEC were cultured in complete culture medium alone or with VEGF (VEGF-A 100 ng/mL) or FGF (FGF2 100 ng/mL). Results from IncuCyte monitoring are expressed as mean ($\pm$ SD; 4 replicate cultures) percentage culture confluence (48 hour time point). P = statistical significance of group differences.

retinal cup was incubated (18 hours, room temperature) with goat anti–mouse Sema6A polyclonal antibody (1:25; R&D Systems) and biotinylated isolectin B4 (1:50; Invitrogen). Alexa Fluor 488–conjugated anti–goat IgG (1:2000; Invitrogen) and Alexa Fluor 647–conjugated streptavidin (1:100; Invitrogen) were used for detection (1 hour, room temperature). The stained retinal cup was fixed (4% paraformaldehyde, 20 minutes, room temperature), and flat-mounted with Vectashield containing DAPI. Retinas were imaged through a Zeiss LSM710 confocal microscope.

Isolated choroids[30] were stained with Alexa Fluor 594–conjugated isolectinB4 (IB4; Invitrogen), and flat-mounted in Aquamount with sclera facing down. Neovascular areas stained by IB4 were measured (Axiovision software; Carl Zeiss); the mean neovascular area/eye was calculated from measurements of individual lesions. Matrigel plugs (whole) and tumors were fixed (4% paraformaldehyde in PBS, 1 hour at 4°C), soaked (15% and 30% sucrose), cryopreserved (OCT embedding media; Tissue-Tek) and sectioned (10 μm thickness), as described.[25,27] After blocking (Fc receptor blocker, 1 hour, room temperature; Innovex Bioscience), tissue sections were incubated (18 hours, room temperature) with goat anti–mouse Sema6A (1:50; R&D Systems), rat anti–mouse CD31/PECAM (BD Pharmingen) and rabbit IgG anti-NG2 (Chemicon International); Alexa Fluor 548–conjugated anti–goat IgG (1:400; Molecular Probes), Alexa Fluor 647–conjugated goat anti–rat IgG (1:400; Molecular Probes), and Alexa Fluor–conjugated goat anti–rabbit IgG (1:400; Molecular Probes) were used for detection. DAPI (Invitrogen; 1:2000) was used to visualize nuclei. Tumor and Matrigel sections were imaged with an Axiovert 200 fluorescence microscope (Carl Zeiss) as described[27]; images digitalized using the Volocity imaging program (PerkinElmer). The pseudo-colored images were converted to TIF files, exported to Adobe Photoshop, and overlaid. Images from fluorescent CD31 and DAPI staining were quantified (ImageJ Version 1.46 software, NIH). Pixel values for CD31 and DAPI fluorescence were from the entire tissue section (tumor or matrigel plug). Ratios of CD31 pixel count/DAPI pixel count were calculated from each section to derive a relative mean CD31 pixel count. Relative mean pixel counts from groups of tissue sections were averaged.

Statistical analysis

Group differences were measured by 2-tailed Student t test. P values less than .05 were considered significant.

Results

Sema6A promotes endothelial cell viability and VEGF-A–induced growth

Primary HUVECs express Sema6A mRNA, which can be effectively silenced (1 vs 0.167 $\pm$ 0.07, n = 4; P = .001) using specific lentiviral shRNAs (Figure 1A). We found that a higher proportion of _Sema6A_-silenced cells were apoptotic or dead compared with control cells transduced 72 hours earlier with the control vector (Figure 1B, representative results; in 4 experiments the % cells apoptotic/dead was 44.9 $\pm$ 3.3 in _Sema6A_-silenced cultures as opposed to 17.18 $\pm$ 2.8 in control; P = .01). Specificity of the association between _Sema6A_ silencing and cell apoptosis/death was confirmed using a different shRNA (supplemental Figure 1A-B, available on the _Blood_ Web site; see the Supplemental Materials link at the top of the online article). We recovered the cells that survived after 72 hours, and examined cell growth. Time-lapse IncuCyte imaging over 90 hours showed that _Sema6A_-silenced HUVECs grew at a lower rate than control cells (Figure 1C).

After 7-day-culture with puromycin, we recovered HUVEC in which _Sema6A_ expression was reduced compared with control cells (Figure 1A). Using these cells, we confirmed that _Sema6A_-silenced endothelial cells die at a significantly higher rate than control cells (Figure 1D: group results expressed as means $\pm$ SEM,

5 experiments). By immunostaining, 31.8% of Sema6A-deficient HUVECs and 8.3% of control HUVECs displayed cleaved caspase-3 (Figure 1E).

All HUVEC cultures were supplemented with ECGS (endothelial cell growth supplement that contains basic and acidic FGFs). Nonetheless, we examined whether additional VEGF-A or FGF2 could limit cell death and promote cell growth in *Sema6A*-silenced HUVEC. VEGF-A increased the proliferation of *Sema6A*-silenced cells to a lower degree (% confluence 25.96 ± 11.62 vs 54.23 ± 1.23; $P < .001$) than that of control cells (Figure 1F). FGF2 did not significantly increase the proliferation of control and *Sema6A*-silenced cells (27.5 ± 9.32 vs 17.97 ± 9.63 $P = .064$), attributable to the high FGF2 content in the ECGS supplement (Figure 1F). Thus, Sema6A-deficient endothelial cells die at an abnormally high rate, and respond poorly to exogenous VEGF-A growth stimulation.

Relationship between Sema6A deficiency and VEGFR2 expression

We examined whether reduced VEGFR2 expression levels might underlie reduced proliferation to exogenous VEGF-A in *Sema6A*-silenced endothelial cells. By flow cytometry, we found that 72 hours after infection with Sema6A shRNAs, HUVEC display reduced levels of VEGFR2 in comparison to control cells (Figure 2A, representative results; in 4 experiments, $77.8 \pm 4.3\%$ of control cells displayed high VEGFR2 levels as opposed to only $53.1 \pm 3.5\%$ of *Sema6A*-silenced cells; $P = .008$). Because 72 hours after infection a substantial proportion of *Sema6A*-silenced cells detach and die (the sequence of these events was not investigated), we examined whether low Sema6A expression and low VEGFR2 expression coincided with the occurrence of cell death. The *Sema6A*-silenced HUVECs that had detached from the dish displayed lower expression of Sema6A mRNA (Figure 2B) and VEGFR2 protein (Figure 2C), and increased expression of cleaved caspase 3 (Figure 2C) compared with the cells that continued to adhere. We confirmed that the *Sema6A*-silenced cells that had detached exhibited reduced expression of VEGFR2 in comparison to the cells that continued to adhere (supplemental Figure 2A). In contrast to the reduction of VEGFR2 protein, levels of Neuropilin-1 protein were similar in control and *Sema6A*-silenced HUVECs (supplemental Figure 2B).

These results suggested that cell death induced by *Sema6A* silencing is linked to reduced VEGFR2 expression. To confirm this, we examined whether reduced VEGFR2 expression persisted in HUVEC stably silenced of *Sema6A*, as they survived 7-day puromycin selection. By flow cytometry (Figure 2D; representative experiment; in 5 experiments, 17.6% of *Sema6A*-silenced cells expressed high levels VEGFR2, as opposed to 62.8% of controls; $P = .027$), quantitative PCR (Figure 2E; 1 versus 0.253 ± 0.098, 4 experiments; $P = .005$) and immunoblotting (Figure 2F) we found that *Sema6A*-silenced HUVECs express lower levels of VEGFR2 mRNA and protein in comparison to control cells.

Sema6A can signal through its identified plexinA2 and plexinA4 receptors and potentially through its intracellular domain, albeit this pathway remains poorly defined.[15,18] We examined VEGFR2 expression in HUVEC subjected to *Sema6A, plexinA2, plexinA4,* or *plexinA2* plus *plexinA4* silencing. If plexinA2 and plexinA4 receptors mediate VEGFR2 regulation by Sema6A, silencing expression of these receptors should reduce VEGFR2 expression similar to *Sema6A* silencing. We found that the silencing of *plexinA2* and *plexinA4* individually or together did not reduce the levels of VEGFR2 mRNA and protein in HUVECs, whereas the

silencing of *VEGFR2* or *Sema6A* did (Figure 2G-H), providing evidence that plexinA2 and plexinA4 do not mediate Sema6A regulation of VEGFR2 expression. In additional experiments, we used recombinant soluble Sema6A-Fc. As shown (Figure 2I), Sema6A-Fc specifically and dose-dependently rescued VEGFR2 expression in *Sema6A*-silenced HUVECs but not in control HUVECs, providing evidence that Sema6A-Fc can mimic endogenous Sema6A in the regulation of VEGFR2 expression.

Impaired VEGFR2 signaling in Sema6A-deficient endothelial cells

We examined VEGFR2 signaling in *Sema6A*-silenced HUVECs. In contrast to its activating effects in control cells, VEGF-A (100 ng/mL) induced minimal or no phosphorylation of VEGFR2, Akt, and Erk1/2 in *Sema6A*-silenced HUVECs, as measured by immunoblotting (Figure 3A). Flow cytometry measurements of intracellular phospho-AKT (Figure 3B) and phospho-Erk (Figure 3C) confirmed that Sema6A-deficient HUVECs are defective at signaling in response to VEGF-A. These experiments demonstrate that Sema6A expression is required for VEGFR2 expression and signaling in endothelial cells, and suggested that the loss of VEGFR2 expression and VEGF-A signaling contribute to increased cell death in Sema6A-deficient cells.

FGF2 promotes the survival, proliferation and migration of primary endothelial cells.[32] Because *Sema6A*-silenced HUVEC survive and proliferate less well than control cells in culture medium containing nonlimiting amounts of FGF (Figure 1C), we investigated whether Sema6A regulates FGF2 responses in HUVEC. Expression levels of FGFR1, the main receptor for FGF2 in endothelial cells,[32] are only modestly decreased in Sema6A-deficient cells compared with control cells (Figure 3D; 1 vs 0.73 ± 0.169, 6 experiments; $P = .175$). This contrasts with the marked reduction of VEGFR2 expression in Sema6A-deficient cells (Figure 2D), a difference that we confirmed using a different Sema6A shRNA (supplemental Figure 1C). In addition, *Sema6A*-silenced and control HUVECs displayed similar AKT and Erk phosphorylation in response to FGF2 (after FGF2 starvation; Figure 3E) and flow cytometry (Figure 3F-G), providing evidence that VEGF-A, but not FGF2 signaling, is disrupted in *Sema6A*-silenced endothelial cells.

Sema6A-silenced cells signal normally to FGF2 (Figure 3E-G) but die or proliferate poorly in the presence of FGF2-rich culture medium (Figure 1C), suggesting that additional factor(s) required for endothelial cell growth and survival were missing or altered in these cells. Because previous studies demonstrated an absolute requirement for endogenous VEGF to support endothelial cell survival, which could not be substituted by exogenous VEGF,[33] we examined *VEGFA* expression levels in Sema6A-deficient HUVECs. We found that Sema6A-deficient and control HUVEC express similar levels of VEGF-A mRNA (Figure 4A; 1 vs 1.2 ± 0.15, 4 experiments; $P = .7$), suggesting that a reduction in VEGF-A production was unlikely the cause of increased death and reduced proliferation in *Sema6A*-silenced cells. However, because Sema6A-deficient HUVECs have reduced VEGFR2 expression and signaling, we examined the possibility that VEGFR2 deficiency might account for defective responsiveness to endogenous VEGF-A. First, we tested whether blocking VEGFR2 signaling in normal endothelial cells reduces cell survival. Sorafenib (5-10μM), a small molecule inhibitor of tyrosine protein kinases, including VEGFR2, effectively blocked VEGF-A signaling in HUVECs (Figure 4B). Sorafenib (10μM) also induced cell death in normal endothelial cells, in spite of the fact that the cells were cultured in
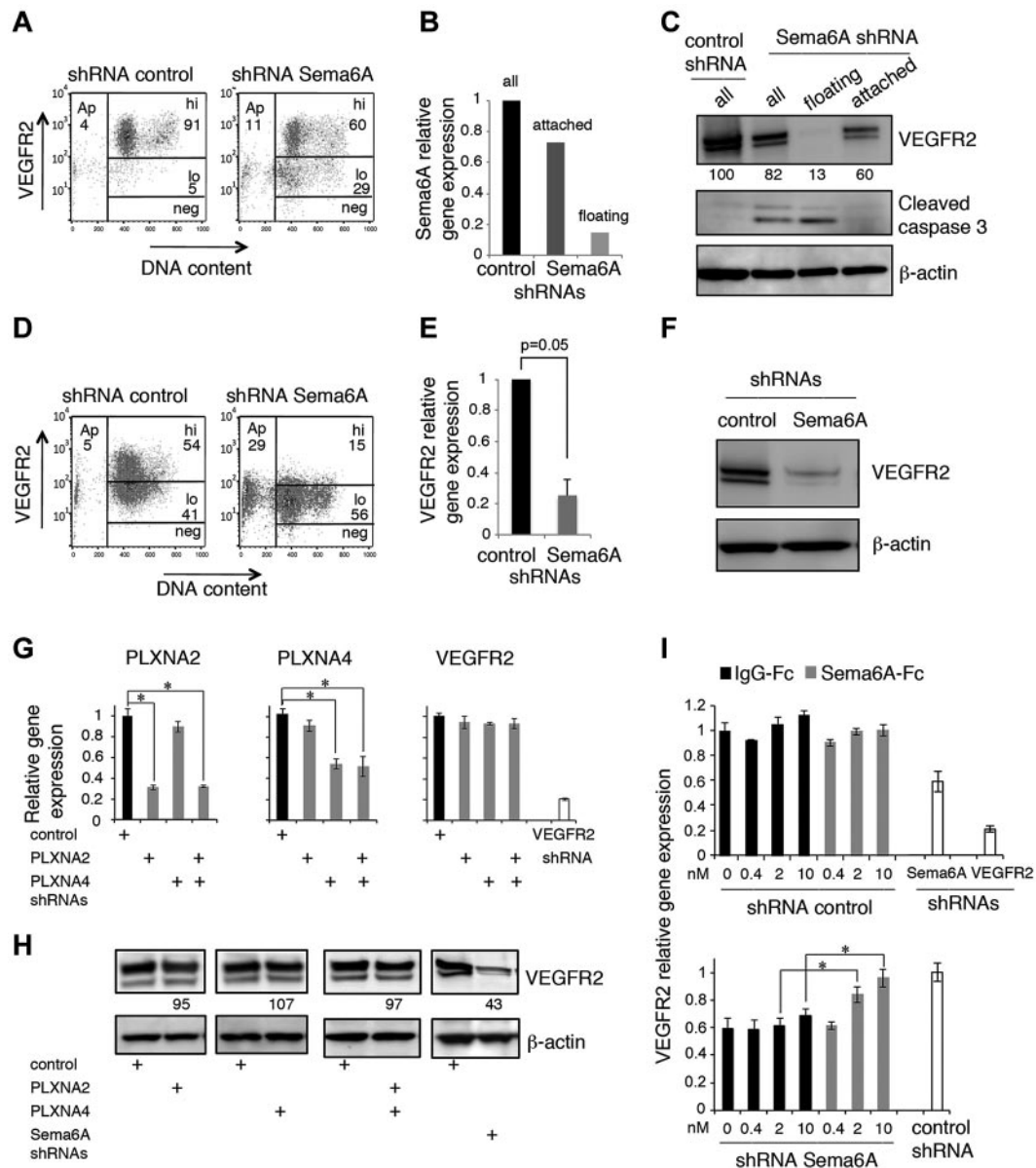
Figure 2. *Sema6A* silencing decreases VEGFR2 levels in endothelial cells. (A) VEGFR2 levels in HUVECs 72 hours after infection with control or Sema6A shRNA. Representative flow cytometry profiles display VEGFR2 levels (hi indicates high; lo, low; and neg, negative) as a function of DNA content (DAPI staining after cell permeabilization); Ap indicates apoptotic cells. (B) Relative levels of Sema6A expression in HUVEC control (control shRNA) and *Sema6A*-silenced (Sema6A shRNA) attached or floating 72 hours after infection measured by quantitative PCR. (C) Levels of VEGFR2 and cleaved caspase3 in cell lysates of HUVECs 72 hours after infection with control or Sema6A shRNA detected by immunoblotting; β-actin was used as loading control. The *Sema6A*-silenced cells were examined as attached, floating, and all cells. Normalized (VEGFR2/β-actin) band intensity values are displayed. After infection with control or Sema6A shRNAs and 7-day puromycin selection, HUVECs were tested for VEGFR2 expression by flow cytometry (D) and quantitative PCR (E). The results of PCR are expressed as mean gene expression ($\pm$ SEM; n = 5) relative to control. (F) VEGFR2 protein was evaluated by immunoblotting in cell lysates of *Sema6A*-silenced and control HUVECs (after 7-day puromycin selection). (G) Relative levels of plexinA2 (PLXNA2), plexinA4 (PLXNA4), and VEGFR2 expression in HUVEC control (shRNA control) and in HUVECs subjected to shRNA knockdown of *PLXNA2*, *PLXNA4*, *PLXNA2*+*PLXNA4*, or *VEGFR2*. The results of PCR reflect the means RNA levels ($\pm$ SD; n = 4) relative to control. (H) VEGFR2 levels in cell lysates of HUVEC control (shRNA control) and in HUVECs with shRNA knockdown of *PLXNA2*, *PLXNA4*, *PLXNA2*+*PLXNA4*, or *Sema6A*. Relative band intensities values (normalized to β-actin) are displayed. (I) Relative levels of VEGFR2 mRNA in attached control (shRNA control) and *Sema6A*-silenced (shRNA Sema6A) HUVECs supplemented with IgG1-Fc or recombinant Sema6A-Fc (0.4-10nM). *VEGFR2*-silenced (shRNA VEGFR2) HUVEC were used as a control (*$P < .001$).

complete culture medium containing nonlimiting amounts of FGF2 (Figure 4C, representative results; in 3 experiments the % apoptotic cells was 21.6 ± 2.0 in sorafenib-treated cultures as opposed to 11.6 ± 1.8 in control cultures, $P = .03$). Second, we tested the effects of silencing *VEGFR2* in HUVECs. The silencing of *VEGFR2* expression was associated with expression of cleaved caspase 3 (Figure 4D) and with a significant reduction in cell viability (Figure 4E-F). Third, we compared VEGFR2 phosphory-lation and total levels in *Sema6A*-silenced or *VEGFA*-silenced

HUVECs (Figures 4G-H). As previously reported,[33] addition of the phosphatase inhibitor Na_3VO_4 revealed the presence of constitu-tively phosphorylated VEGFR2 in HUVECs (Figure 4H left panels). This is attributable to stimulation from endogenous VEGF-A as it was not reduced by neutralizing antibodies to VEGF-A (avastin 10 μg/mL; Figure 4H left panels) but was abrogated by sorafenib (2mM; Figure 4H left panels) and by *VEGFA* silencing, which reduces VEGF-A expression (Figure 4H right panels and G). The silencing of *Sema6A* reduced levels of
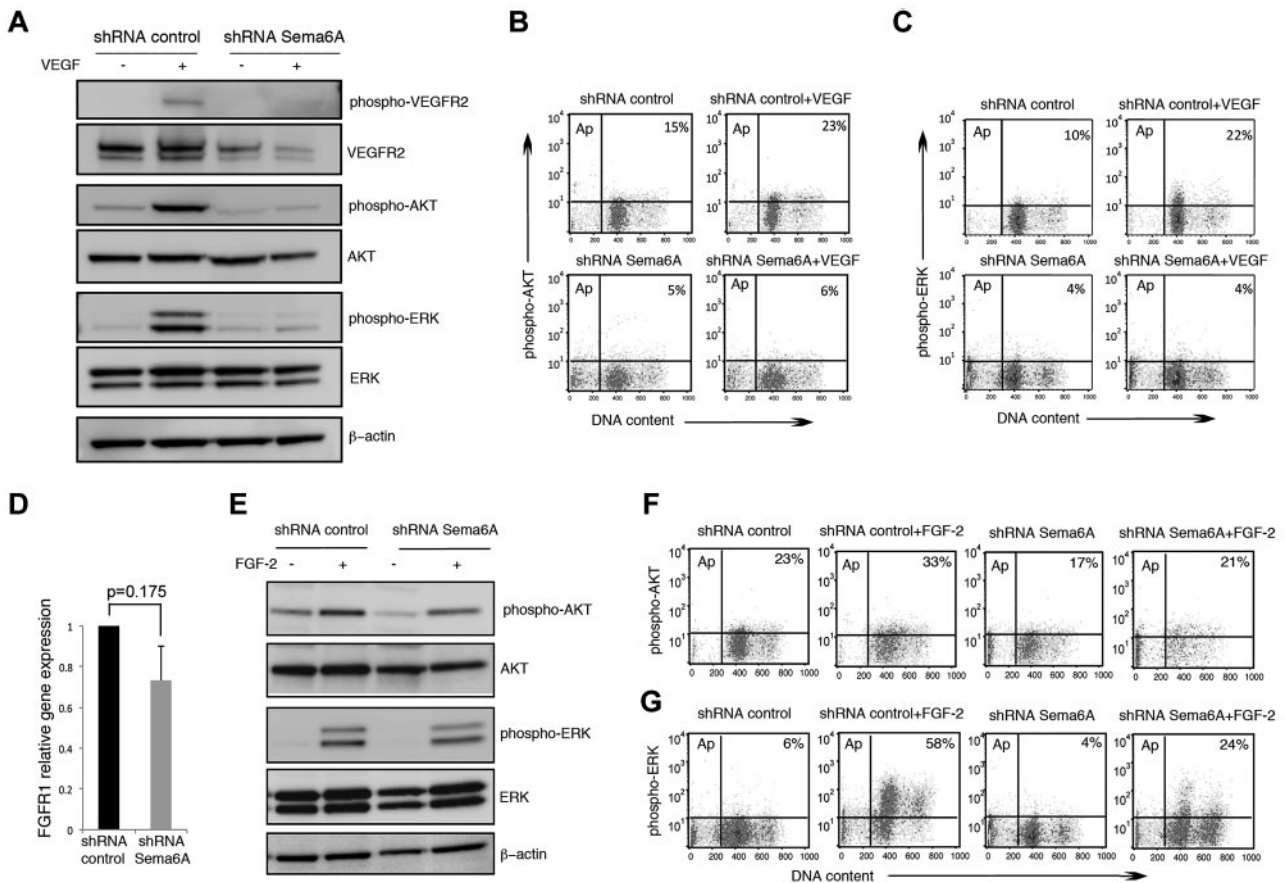
Figure 3. VEGF-A and FGF2 signaling in *Sema6A*-silenced endothelial cells. (A) Control and *Sema6A*-silenced HUVECs were incubated 15 minutes with VEGF-A (100 ng/mL). Cell lysates were tested for phosphorylated and total VEGFR2, AKT, and ERK1/2; β-actin staining was used as a loading control. (B) Intracellular phospho-AKT and (C) intracellular phospho-ERK were analyzed by flow cytometry under the same experimental conditions of A. The results represent the relative percentage of phospho-AKT and phosphor-ERK positive cells (representative experiments). (D) FGFR1 gene expression was measured by quantitative PCR in *Sema6A*-silenced and control HUVECs. The results reflect the mean (± SEM; n = 6) mRNA levels relative to control. (E) *Sema6A*-silenced and control HUVECs were incubated (15 minutes) with FGF2 (100 ng/mL). Phosphorylation levels of AKT and ERK1/2 were assessed in the cell lysates by Western blotting. (F) Intracellular phospho-AKT and (G) intracellular phospho-ERK were analyzed by flow cytometry under the same experimental conditions of E.

endogenously phosphorylated VEGFR2 and the levels of total VEGFR2 (Figure 4H middle panels). In addition, endogenous VEGFR2 phosphorylation is not observed in *VEGFA*-silenced cells in the presence of Na_3VO_4 (Figure 4G right panels). Neutralizing antibodies to VEGF-A minimally affected the levels of VEGFR2 and phospho-VEGFR2 in *Sema6A*-silenced cells (Figure 4H middle panels), providing evidence that Sema6A regulates VEGFR2 activity even in response to the endogenous VEGF-A. Together, these results demonstrate that Sema6A modulates endothelial cell survival and growth by regulating VEGFR2 expression and function.

Sema6A modulates hyaloid and retinal vessel development/remodeling

We used the previously described Sema6A-null mice to examine whether Sema6A displays similar activities in vivo. These mutant mice carry a gene-trap insertion in the Sema6A gene resulting in the fusion of the extracellular domain of Sema6A to the TM-β-geo reporter.[22-24] Such Sema6A fusion proteins are sequestered in the endoplasmic reticulum and in multiple inclusion bodies (probably lysosomes) and thus the mice are phenotypically Sema6A-null[22-24]; they are born alive and reach adulthood, but display developmental defects in the nervous system, many of which are compensated in the adult mouse.[22,24,34-37] No defects in vascular development were previously described.

The eye contains 3 vascular beds, the transient hyaloid vasculature, the retinal vessels, and the choroidal vessels.[38] Hyaloid vessels, an arterial vascular network that supports embryonic growth of the eye, is fully developed at birth and regresses as the retinal vasculature forms.[39] We found that Sema6A is broadly expressed in hyaloid vessels from 5-day-old (P5) wild-type, but not Sema6A-null mice (Figure 5A). Interestingly, hyaloid vessels from P4 Sema6A-null mice differed from controls in displaying reduced network complexity (Figure 5B), reflected by a significant (136.67 ± 6.17 vs 218.5 ± 9.04, P = .001) reduction in the number of branching points in littermates (n = 3 littermates; Figure 5C). Some of the Sema6A-null hyaloid vessels appeared as cords of endothelial cells joined by thin cytoplasmic extensions, suggesting the occurrence of increased cell death (Figure 5B). Consistent with the results from *Sema6A* silencing in HUVECs, VEGFR2 protein levels were reduced in extracts from P5 Sema6A-null mice compared with wild-type and heterozygote controls (Figure 5D). Immunostaining for cleaved caspase 3 confirmed the occurrence of increased cell death in Sema6A-deficient hyaloid vessels compared with wild-type control (Figure 5E). These results provide evidence that Sema6A expression contributes to generate/maintain complexity and promote viability in hyaloid vessels.

Retinal vessels begin to develop as the hyaloid vessels regress[38,40] forming a network sprouting from the optic nerve and radiating outward in the superficial retinal layer from this central
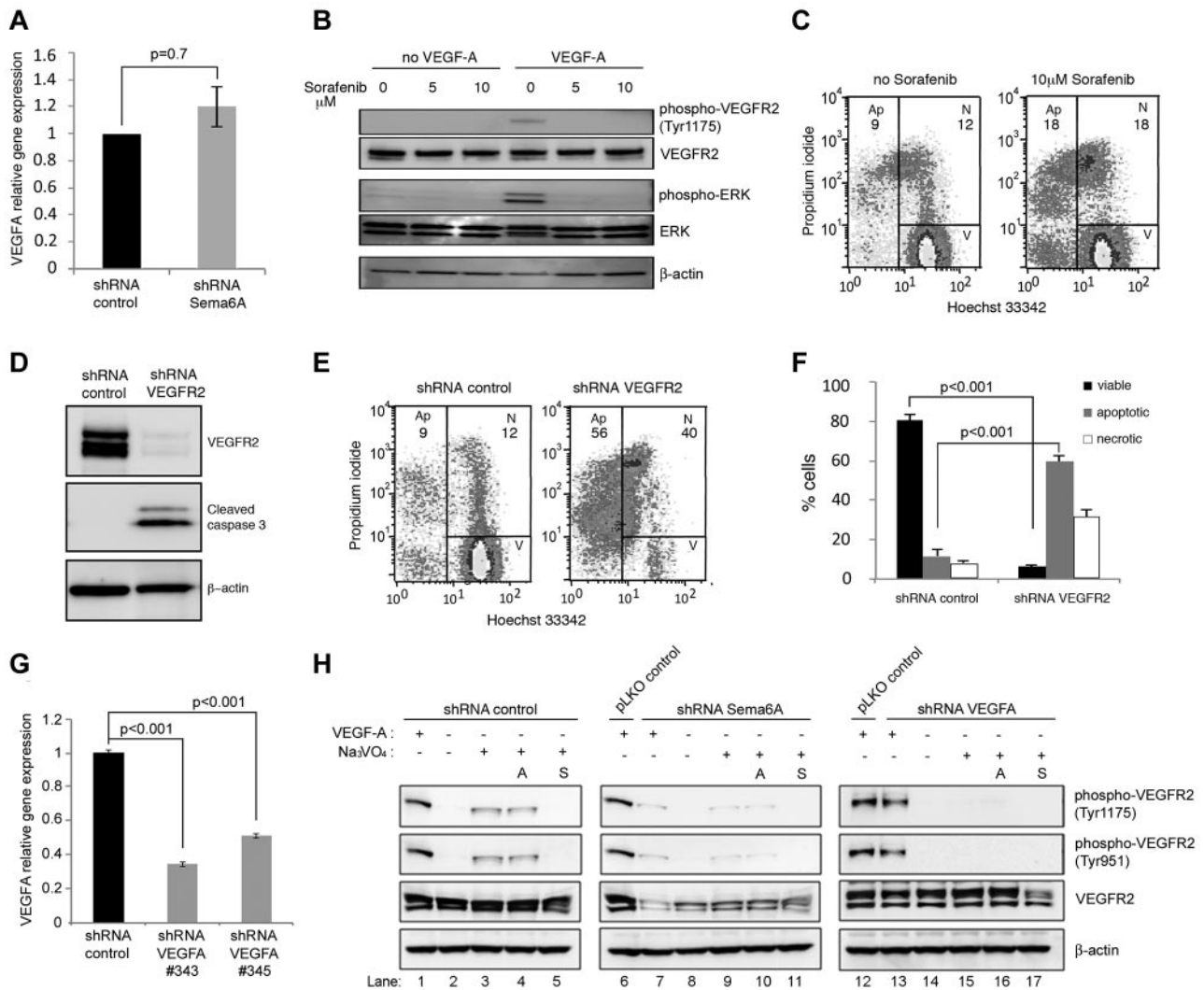
Figure 4. Endothelial cells require VEGF signaling for survival. (A) *VEGFA* gene expression in *Sema6A*-silenced and control HUVECs was measured by quantitative PCR. The results reflect the mean (± SEM; n = 4) relative mRNA levels. (B) HUVECs were incubated (2 hours) with Sorefanib at the indicated concentrations and then treated with VEGF-A (100 ng/mL; 15 minutes). Cells lysates were tested for VEGFR2 and ERK phosphorylation by immunoblotting. (C) Cell death was measured by flow cytometry in HUVECs incubated (18 hours) with medium only or medium supplemented with Sorafenib (10μM). (D) HUVECs were infected with control (shRNA control) or *VEGFR2* silencing lentivirus (shRNA VEGFR2). Cell lysates were evaluated for VEGFR2 and cleaved caspase 3 by Western blotting. (E) Cell death in *VEGFR2*-silenced and control HUVECs was measured by flow cytometry (representative results). (F) The bar graph shows the percentage viable, apoptotic and necrotic *VEGFR2*-silenced and control HUVECs from 4 independent experiments (± SEM; *P* values reflect statistical significance of group differences). (G) *VEGFA* gene expression in *VEGFA*-silenced (VEGFA shRNA 343 or 345) and control HUVEC measured by quantitative PCR. (H) Control (shRNA control), *Sema6A*-silenced (shRNA Sema6A) or *VEGFA*-silenced (shRNA VEGFA) HUVEC were cultured for 6 hours in EBM-2 medium supplemented with FGF2, EGF, and IGF-1 from EGM-2 BulletKit. Avastin (A; lanes 4, 10, and 16) was added at 10 μg/mL; Sorafenib (S; lanes 5, 11, and 17) was added at 2μM; and Na₃VO₄ (lanes 3-5, 9-11, 15-17) was added at 100μM. Cells were stimulated with exogenous VEGF-A (100 ng/mL) for 5 minutes. Cell lysates were immunoblotted for phosphorylated VEGFR2 (tyrosine 1175 or 951), total VEGFR2 and β-actin.

point. Retinal vessels reach the retinal periphery during the first week of life in mice. We compared the retinal vessel network in Sema6A-null mice and wild-type P4 littermates. Strikingly, the extension of the vascular network from the optic nerve to the periphery was significantly (21.35 ± 1.12 vs 30.26 ± 2.67, *P* = .011) reduced in Sema6A-null retinas compared with the wild-type littermates (n = 7 littermates; Figure 6A-B). By contrast, the network complexity (as reflected by the number of retinal vessels branching points) was similar (490.4 ± 13.62 vs 494.11 ± 29.27, *P* = .92; Figure 6C). This difference in retinal vessel extension between wild-type and Sema6A-null retinas was no longer detected by P8 (not shown), suggesting that Sema6A is a time-dependent contributor of physiologic retinal angiogenesis. By immunohistochemistry, Sema6A is detected in the retinal vessels from wild-type, but not Sema6A-null mice as it coincides with isolectinB4 staining, including the filopodial extensions of "tip" cells (Figures 6D-E).

Sema6A is also detected independently of isolectinB4 staining (Figure 6E), and is attributable to reactivity to the neuronal retina, particularly in the ganglion cell layer (supplemental Figure 3).

Sema6A modulates pathologic angiogenesis and tumor growth

The choroidal vessel network consists of a highly fenestrated capillary bed arising from the posterior ciliary arteries and draining into the vortex veins, which provides support to the avascular outer retinal layers, including the photoreceptors.[38,41] Because this network is established at birth, we examined injury-induced choroidal vessel neovascularization after inducing choroidal neovascularization (CNV) by laser injury to the Bruch membrane, the innermost layer of the choroid.[30,42,43] We found that the angiogenic response on day 7 after injury, which is associated with Sema6A expression by the angiogenic wild-type vessels (not shown), was significantly (*P* = .011) reduced in
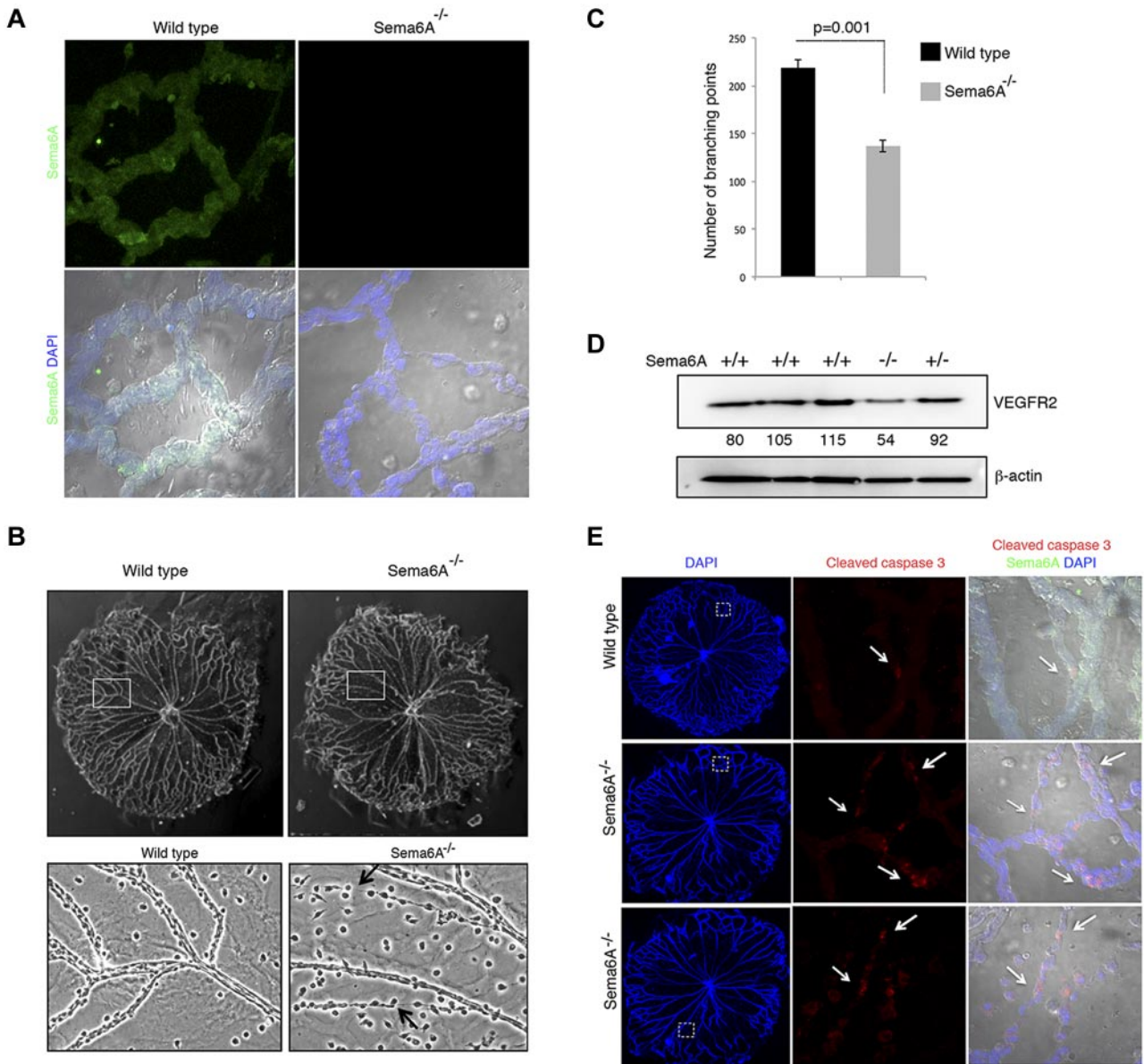
Figure 5. Hyaloid vessels from Sema6A$^{-/-}$ mice and wild-type littermates. (A) Isolated hyaloid vessels from 4-day-old (P4) Sema6A-null and wild-type littermates were immunostained for Sema6A. Nuclei are visualized with DAPI. Representative images. (B) Morphology of hyaloid vessels isolated from P4 wild-type and Sema6A-null littermates; magnification of wild-type and Sema6A-null hyaloid vessels from corresponding areas outlined in the top panels. Representative images. (C) Number of branching points in hyaloid vessels isolated from wild-type and Sema6A-null littermates (n = 3, paired littermates; SEM; p reflects the statistical significance of group difference. (D) Protein extracts of isolated hyaloid vessels from wild-type (+/+), Sema6A heterozygote (+/−) and Sema6A-null (−/−) P5 mice were tested for VEGFR2 and β-actin by immunoblotting. Normalized (VEGFR2/β-actin) band intensity values are shown. (E) Isolated hyaloid vessels from P5 wild-type and Sema6A-null mice were immunostained for cleaved caspase 3 and Sema6A. Nuclei are visualized with DAPI. Comparable hyaloid vessel areas are magnified in the middle and right panels. Images on the right panels are from DIC (differential interference contrast microscopy).

Sema6A-null mice compared with the littermate controls (n = 8; Figure 7A-B).

We further used an in vivo model in which angiogenesis is induced in adult mice by subcutaneous inoculation of the proangiogenic factors VEGF-A and FGF2 within a mixture of extracellular matrix proteins (matrigel). The plugs, removed 7 days after inoculation, were stained for Sema6A, CD31, and NG2 to identify endothelial cells and mural cells, respectively. Plugs from Sema6A-null mice contained a significantly reduced number of CD31-expressing endothelial cells compared with the littermate controls reflective of reduced angiogenesis (Figure 7C-D). Of interest, Sema6A marked the newly formed vessels within the plug from

wild-type mice; as expected, Sema6A was not detected in the plugs of Sema6A-null mice (Figure 7E).

We compared tumor angiogenesis in Sema6A-null mice and wild-type adult littermates by injecting subcutaneously the murine melanoma B16 and LLC/1 carcinoma cells to generate tumors. These tumor cell lines were selected as they are syngeneic to the Sema6A-mutant mice, they are either responsive (B16) or resistant (LLC/1) to VEGF-A neutralization,[44] and differ in levels of expression of Sema6A, plexinA2, and plexinA4 (supplemental Figure 4). Ten days after injection of the tumor cells, we removed all tumors. The weight of B16 and LLC/1 tumors developed in the Sema6A-null mice was significantly reduced compared with those
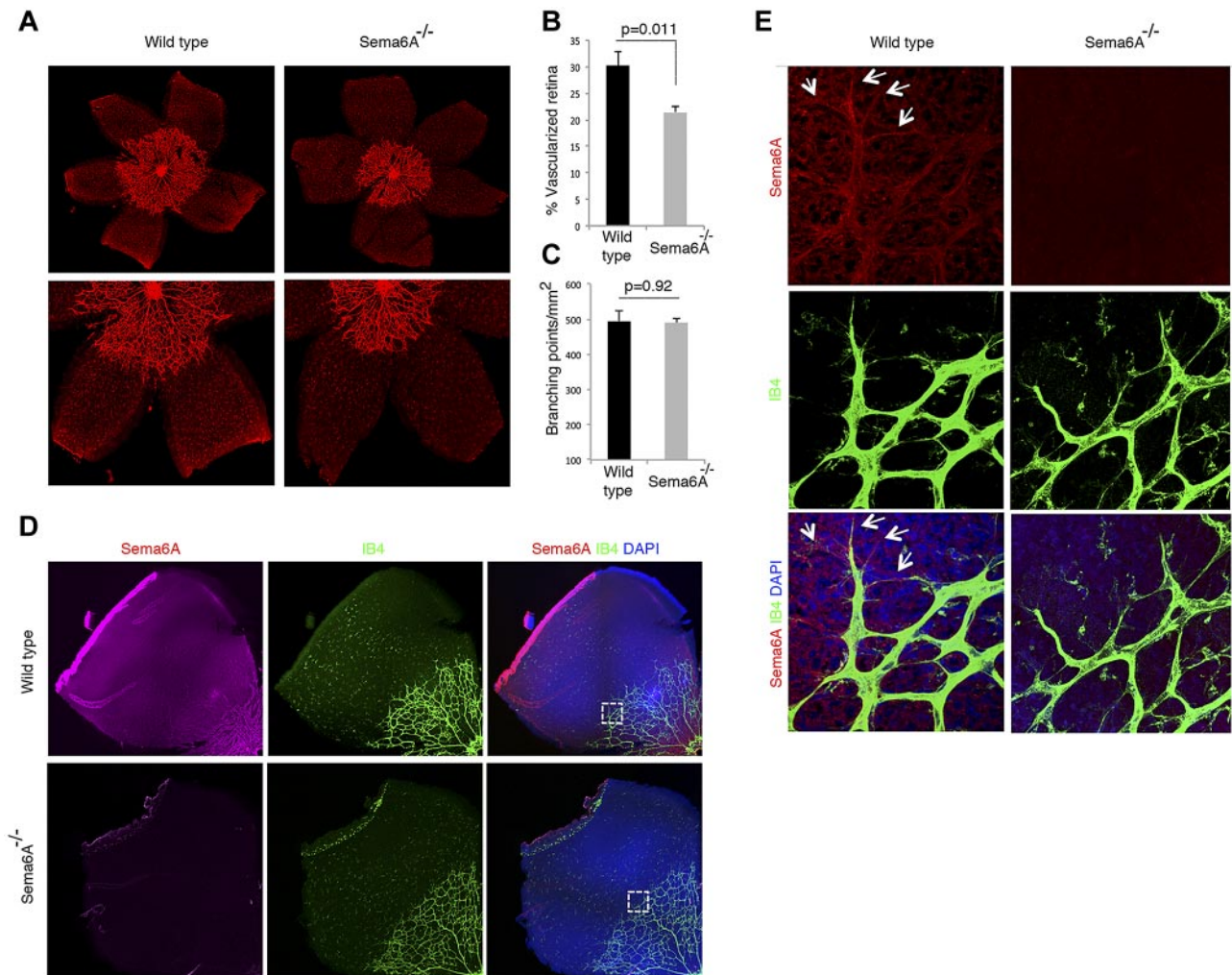
Figure 6. Defective retinal vascularization in Sema6A$^{-/-}$ mice. (A) Retinal whole mounts from paraformaldehyde-fixed eyes of P4 Sema6A-null and wild-type littermates; representative images. (B) Average radial length of retinal vessels from the optic nerve to the periphery was measured in P4 paired littermates (n = 7; mean ± SEM). The results are expressed as percentage retina occupied by vessels. (C) Number of branching points/mm^2 retinal vessels was measured in P4 paired littermates (n = 7; mean ± SEM). (D) Sema6A immunostaining of P4 wild-type and Sema6A-null retinas. Isolectin B4 (IB4) was used for visualization of retinal vessels; nuclei are visualized with DAPI. (E) Magnified section of retina from panel D showing Sema6A expression in wild-type retinal vessels (IB4-positive) and in ganglion cells. The arrows point to endothelial filopodia expressing Sema6A. Comparative images from wild-type and Sema6A-null tissues were obtained and processed by using the same settings.

that developed in wild-type littermates (Figure 7F-G). Microscopic visualization of the B16 and LLC/1 tumor tissues after immunostaining for CD31 and NG2 suggested and measurement of CD31-positive vessel density confirmed that tumors arising in Sema6A-null mice were less vascularized compared with those from wild-type littermates (Figure 7H-K). These results show that the angiogenic response to tumor challenge is reduced in Sema6A-null mice, providing evidence that Sema6A supports tumor angiogenesis.

Discussion

Sema6A and its receptors plexinA2 and plexinA4 have been extensively characterized for their essential roles in neuronal developmental processes,[22,24,34-37] but their roles in vascular development and endothelial cell function remain largely unexplored. Here, we demonstrate that Sema6A contributes to vascular development and to angiogenesis after maturity by modulating VEGFR2 signaling in endothelial cells.

We used the homozygous Sema6A$^{-/-}$ mice generated by a gene-trap mutation in the Sema6A locus[22] to look for developmen-

tal vascular defects. Sema6A-deficient mice are born alive without overt defects and survive to adulthood, but display developmental defects in the nervous system,[15,22,24,34-37] some of which normalize after birth in spite of persistent Sema6A-deficiency.[45] Our analysis finds that Sema6A-deficient mice also display vascular developmental defects that were not previously described. Hyaloid vessels, which provide a temporary blood supply to the eye, display reduced complexity and regress abnormally rapidly in Sema6A-null mice. Retinal vessels develop abnormally slowly in Sema6A-deficient mice, but eventually reach full development. Consistent with Sema6A contributing to their development/remodeling, hyaloid vessels and developing retinal vessels express Sema6A, as we show here, but fully developed retinal vessels do not (not shown). A similar modulation of Sema6A expression was observed in the hippocampus zone CA3 (Cornu Ammonis): high at birth, but absent by P10[25].

Because Sema6A-deficient mice normally survive to adulthood, we tested whether Sema6A plays a role in adult angiogenesis. Our analysis shows that failure to express Sema6A, normally detected in angiogenic endothelium, impairs tumor angiogenesis, laser-induced choroidal angiogenesis, and growth factor-induced matrigel-supported angiogenesis. In all cases, the angiogenic response was
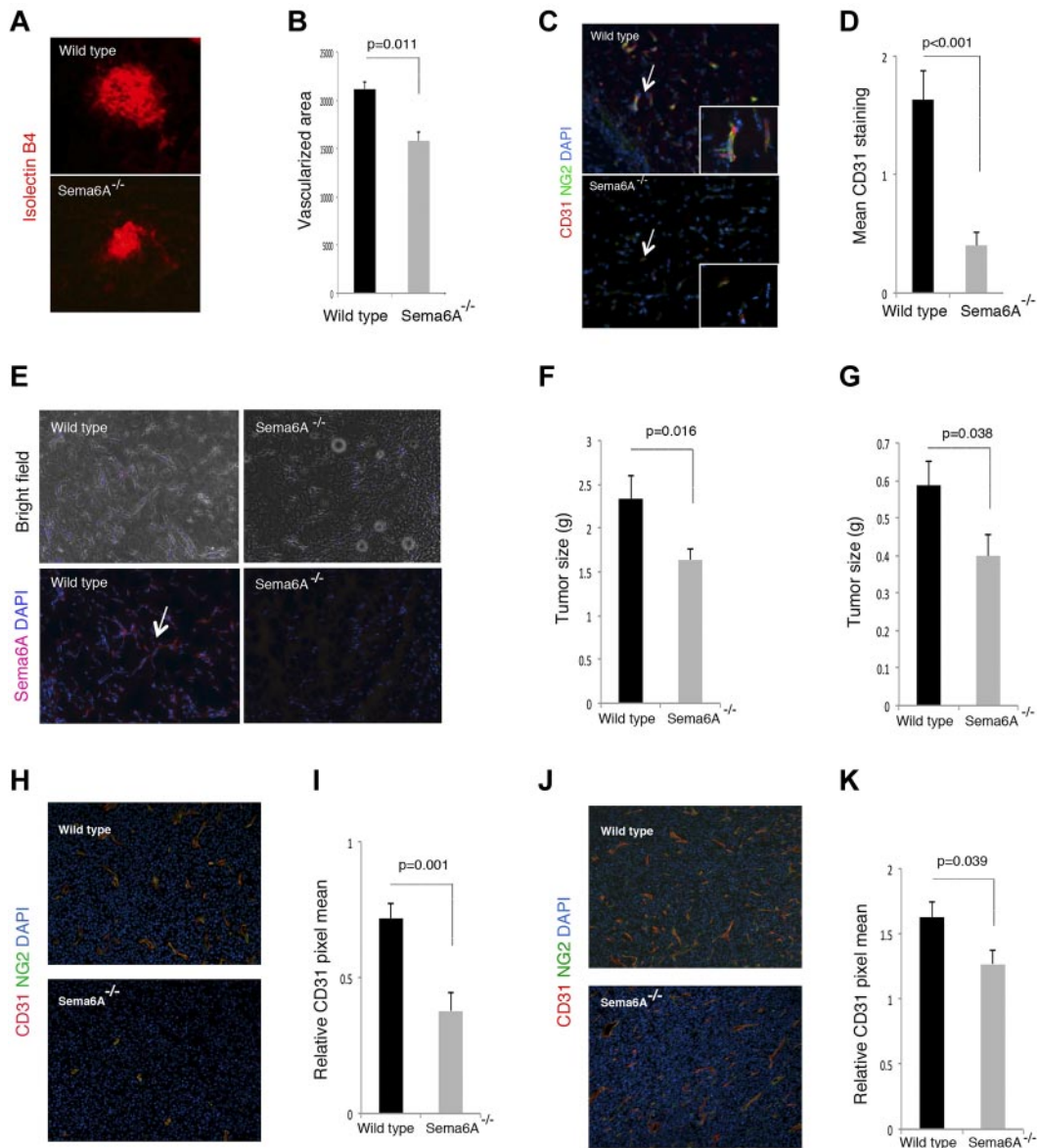
Figure 7. Choroidal, Matrigel-supported and tumor neovascularization in Sema6A⁻/⁻ and wild-type mice. (A) Choroidal neovascularization was evaluated on day 7 after laser injury to the Bruch membrane; representative images of injured areas in representative wild-type and Sema6A-null littermates (6 weeks old); isolectinB4 staining. (B) Quantitative analysis of choroidal neovascularization 7 days after laser injury to the Bruch membrane in groups of wild-type and Sema6A-mutant mice (5 to 6 weeks old). The area occupied by vessels was measured after staining eye wholemount with isolectin B4; the results reflect the group means (n = 8; mean ± SEM; p reflects the statistical significance of group difference). (C) Matrigel plugs containing VEFGA (150 ng/mL), FGF2 (150 ng/mL), and heparin (0.5 mg/mL) were produced subcutaneously in wild-type and in Sema6A⁻/⁻ mice (5 weeks old); plugs were removed after 7 days, processed for histology, and stained for CD31 and NG2. Representative images: the arrow points to a vessel within the matrigel plug, magnified in the inset. (D) Quantative analysis of matrigel neovascularization in groups of wild-type and in Sema6A⁻/⁻ mice (5 to 6 weeks old; 5/group) based on CD31 positive area. (E) Sema6A immunostaining of representative Matrigel plugs from wild-type and Sema6A⁻/⁻ mice. Nuclei are detected with DAPI. Corresponding bright field images are shown in the top panels. (F) B16 murine melanoma and (G) LLC/1 Lewis lung murine carcinoma cells (10 × 10⁶) were injected subcutaneously in groups of wild-type and Sema6A⁻/⁻ mice. The tumors were removed after 10 days (B16) or 12 days (LLC/1) and weighed. The bar graphs represent the mean (n = 14/group; +/− SEM) tumor weight/group. CD31 and NG2 immunostaining in B16 (H-I) and LLC/1 (J-K) tumor tissues. Representative images of immunostaining are shown in (H) and (J). The bar graphs in (I) and (K) represent the mean CD31 staining (area of CD31 staining/unit area of tumor; n = 14/group; +/− SEM). The P values reflect the statistical significance of group differences.

dampened, without overt morphologic differences in the new vessels. Thus, developmental angiogenesis in the retina and adult angiogenesis appear to be similarly dependent on Sema6A function. Consistent with a role of Sema6A in angiogenesis, it was previously reported that Sema6A is expressed at high levels in the vascular placenta[46] and in highly vascularized tumors, but is otherwise low in the normal adjacent tissues.[19]

Why are developmental and adult angiogenesis compromised with Sema6A-deficiency? We find that VEGFR2 signaling is compromised in *Sema6A*-silenced endothelial cells, and this defect deprives endothelial cells of autocrine VEGF/VEGFR2 signaling, which is critical to the maintenance of endothelial cell survival and vascular homeostasis.[33] Sema6A-deficient endothelial cells express normal levels of VEGF-A, but endogenous VEGF is ineffective at promoting cell survival without functional VEGFR signaling.[33] This requirement for autocrine VEGFR2 phosphorylation[33] is not overcome by exogenous FGF2, which signals normally in Sema6A-deficient endothelial cells, or by exogenous VEGF-A. Consistent

with this, we find that the silencing of *VEGFR2* alone or the inhibition of VEGFR signaling promotes endothelial cell death, even in the presence of exogenous FGF2 or VEGF-A. In addition, the silencing of *VEGFA* and the silencing of *Sema6A* similarly reduced autocrine VEGFR2 phosphorylation, indicating that Sema6A regulates VEGFR2 activity in response to exogenous and endogenous VEGF.

Recently, *plexinA4* silencing prevented FGF2 and VEGF-A signaling in endothelial cells attributed to a deficiency of Sema6B signaling.[20] Because plexinA2 and plexinA4 are the 2 known Sema6A receptors,[36,47] we examined whether the effects of *Sema6A* silencing may derive from removal of constitutive plexinA2 and plexinA4 signaling. The silencing of *plexinA2*, *plexinA4*, or both receptors together did not reduce VEGFR2 expression, providing evidence that these receptors are not mediators of Sema6A-induced VEGFR2 regulation and suggesting that other Sema6A receptors might exist. Interestingly, recombinant Sema6A-Fc specifically and dose-dependently rescued VEGFR2 expression in HUVECs subjected to silencing of endogenous *Sema6A*. It is possible that Sema6A-Fc may activate Sema6A receptors yet to be defined or that it may induce retrograde Sema6A signaling. Previously, Sema6A-1, a variant semaphorin6 with 93% amino acid identity to murine Sema6A, was reported to bind to EVL (Ena/VASP-like protein), a member of the Ena/VASP (enabled/vasodilator-stimulated phosphoprotein) protein family that regulates cytoskeleton dynamics, suggesting that transmembrane semaphorins may signal in reverse.[46] Thus, VEGFR2 deficiency in *Sema6A*-silenced cells could be the result defective Sema6A reverse signaling.

Sema6A was recently identified as a target of the mir-23~27~24 gene cluster[48] and of mirRNA-27a/b.[49] These microRNAs were reported to promote endothelial cell sprouting and angiogenesis,[48,49] and suggested that *Sema6A* silencing may mediate these effects.[49] If so, Sema6A would function as an inhibitor of angiogenesis. Our studies provide direct evidence that Sema6A promotes endothelial cell growth, survival, and angiogenesis. Because miR27 is predicted/known to target many RNAs, including Sprouty2 that modulates MAPK activity induced by VEGF,[48] additional studies will be necessary to discern the contribution of Sema6A to modulation of angiogenesis by miR27.

We demonstrate a critical role of Sema6A in vessel development and adult angiogenesis, and show that Sema6A promotes endothelial cell survival/growth modulating VEGFR2 signaling. Thus, Sema6A emerges as yet another example of a regulator of neuronal and vascular development.[50] Moreover, our findings identify Sema6A as a potential therapeutic target for ocular pathologies stemming from defective remodeling of hyaloid vessels, and for reducing tumor angiogenesis.

Acknowledgments

Authorship

Contribution: M.S., H.O., X.H., D.M., A.K., and G.T. performed and analyzed experiments; O.S. and X.L. provided critical insight and experimental tools; G.T. wrote the paper; and M.S., H.O., D.M., and X.L. revised the paper.

Conflict-of-interest disclosure: The authors declare no competing financial interests.

Correspondence: Hidetaka Ohnuki, Laboratory of Cellular Oncology, CCR, NCI, NIH; Bldg 37, Rm 4124, Bethesda, MD 20892; e-mail: ohnukih@mail.nih.gov.

References

1. Tran TS, Kolodkin AL, Bharadwaj R. Semaphorin regulation of cellular morphology. *Annu Rev Cell Dev Biol.* 2007;23:263-292.

2. Neufeld G, Kessler O. The semaphorins: versatile regulators of tumour progression and tumour angiogenesis. *Nat Rev Cancer.* 2008;8(8):632-645.

3. Capparuccia L, Tamagnone L. Semaphorin signaling in cancer cells and in cells of the tumor microenvironment–two sides of a coin. *J Cell Sci.* 2009;122(Pt 11):1723-1736.

4. Koppel AM, Feiner L, Kobayashi H, Raper JA. A 70 amino acid region within the semaphorin domain activates specific cellular response of semaphorin family members. *Neuron.* 1997; 19(3):531-537.

5. Tran TS, Rubio ME, Clem RL, et al. Secreted semaphorins control spine distribution and morphogenesis in the postnatal CNS. *Nature.* 2009; 462(7276):1065-1069.

6. Franco M, Tamagnone L. Tyrosine phosphorylation in semaphorin signalling: shifting into overdrive. *EMBO Rep.* 2008;9(9):865-871.

7. Takahashi T, Fournier A, Nakamura F, et al. Plexin-neuropilin-1 complexes form functional semaphorin-3A receptors. *Cell.* 1999;99(1):59-69.

8. Miao HQ, Soker S, Feiner L, Alonso JL, Raper JA, Klagsbrun M. Neuropilin-1 mediates collapsin-1/semaphorin III inhibition of endothelial cell motility: functional competition of collapsin-1 and vascular endothelial growth factor-165. *J Cell Biol.* 1999; 146(1):233-242.

9. Serini G, Valdembri D, Zanivan S, et al. Class 3 semaphorins control vascular morphogenesis by inhibiting integrin function. *Nature.* 2003;424(6947): 391-397.

10. Narazaki M, Segarra M, Tosato G. Sulfated polysaccharides identified as inducers of neuropilin-1 internalization and functional inhibition of VEGF165 and semaphorin3A. *Blood.* 2008;111(8):4126-4136.

11. Acevedo LM, Barillas S, Weis SM, Gothert JR, Cheresh DA. Semaphorin 3A suppresses VEGF-mediated angiogenesis yet acts as a vascular permeability factor. *Blood.* 2008;111(5):2674-2680.

12. Maione F, Molla F, Meda C, et al. Semaphorin 3A is an endogenous angiogenesis inhibitor that blocks tumor growth and normalizes tumor vasculature in transgenic mouse models. *J Clin Invest.* 2009;119(11):3356-3372.

13. Vieira JM, Schwarz Q, Ruhrberg C. Selective requirements for NRP1 ligands during neurovascular patterning. *Development.* 2007;134(10):1833-1843.

14. Gu C, Rodriguez ER, Reimert DV, et al. Neuropilin-1 conveys semaphorin and VEGF signaling during neural and cardiovascular development. *Dev Cell.* 2003;5(1):45-57.

15. Suto F, Tsuboi M, Kamiya H, et al. Interactions between plexin-A2, plexin-A4, and semaphorin 6A control lamina-restricted projection of hippocampal mossy fibers. *Neuron.* 2007;53(4):535-547.

16. Tawarayama H, Yoshida Y, Suto F, Mitchell KJ, Fujisawa H. Roles of semaphorin-6B and plexin-A2 in lamina-restricted projection of hippocampal mossy fibers. *J Neurosci.* 2010;30(20): 7049-7060.

17. Sato M, Kitada Y, Tabata T. Larval cells become imaginal cells under the control of homothorax prior to metamorphosis in the Drosophila tracheal system. *Dev Biol.* 2008;318(2):247-257.

18. Suto F, Ito K, Uemura M, et al. Plexin-a4 mediates axon-repulsive activities of both secreted and transmembrane semaphorins and plays roles in nerve fiber guidance. *J Neurosci.* 2005;25(14): 3628-3637.

19. Dhanabal M, Jeffers M, Larochelle WJ. Anti-angiogenic therapy as a cancer treatment paradigm. *Curr Med Chem Anticancer Agents.* 2005; 5(2):115-130.

20. Kigel B, Rabinowicz N, Varshavsky A, Kessler O,

Neufeld G. Plexin-A4 promotes tumor progression and tumor angiogenesis by enhancement of VEGF and bFGF signaling. *Blood.* 2011;118(15): 4285-4296.

21. Catalano A, Lazzarini R, Di Nuzzo S, Orciari S, Procopio A. The plexin-A1 receptor activates vascular endothelial growth factor-receptor 2 and nuclear factor-kappaB to mediate survival and anchorage-independent growth of malignant mesothelioma cells. *Cancer Res.* 2009;69(4):1485-1493.

22. Leighton PA, Mitchell KJ, Goodrich LV, et al. Defining brain wiring patterns and mechanisms through gene trapping in mice. *Nature.* 2001; 410(6825):174-179.

23. Mitchell KJ, Pinson KI, Kelly OG, et al. Functional analysis of secreted and transmembrane proteins critical to mouse development. *Nat Genet.* 2001; 28(3):241-249.

24. Kerjan G, Dolan J, Haumaitre C, et al. The transmembrane semaphorin Sema6A controls cerebellar granule cell migration. *Nature Neurosci.* 2005;8(11):1516-1524.

25. Salvucci O, Maric D, Economopoulou M, et al. EphrinB reverse signaling contributes to endothelial and mural cell assembly into vascular structures. *Blood.* 2009;114(8):1707-1716.

26. Follenzi A, Naldini L. Generation of HIV-1 derived lentiviral vectors. *Methods Enzymol.* 2002;346: 454-465.

27. Segarra M, Williams CK, Sierra Mde L, et al. Dll4 activation of Notch signaling reduces tumor vascularity and inhibits tumor growth. *Blood.* 2008; 112(5):1904-1911.

28. Hamel W, Dazin P, Israel MA. Adaptation of a simple flow cytometric assay to identify different stages during apoptosis. *Cytometry.* 1996;25(2): 173-181.

29. Hillion JA, Takahashi K, Maric D, Ruetzler C, Barker JL, Hallenbeck JM. Development of an ischemic tolerance model in a PC12 cell line. *J Cereb Blood Flow Metab.* 2005;25(2):154-162.

30. Li Y, Zhang F, Nagai N, et al. VEGF-B inhibits apoptosis via VEGFR-1-mediated suppression of the expression of BH3-only protein genes in mice and rats. *J Clin Invest.* 2008;118(3):913-923.

31. Narazaki M, Segarra M, Hou X, Tanaka T, Li X, Tosato G. Oligo-guanosine nucleotide induces neuropilin-1 internalization in endothelial cells and inhibits angiogenesis. *Blood.* 2010;116(16): 3099-3107.

32. Turner N, Grose R. Fibroblast growth factor signalling: from development to cancer. *Nature Rev Cancer.* 2010;10(2):116-129.

33. Lee S, Chen TT, Barber CL, et al. Autocrine VEGF signaling is required for vascular homeostasis. *Cell.* 2007;130(4):691-703.

34. Faulkner RL, Low LK, Liu XB, Coble J, Jones EG, Cheng HJ. Dorsal turning of motor corticospinal axons at the pyramidal decussation requires plexin signaling. *Neural Dev.* 2008;3:21.

35. Rünker AE, Little GE, Suto F, Fujisawa H, Mitchell KJ. Semaphorin-6A controls guidance of corticospinal tract axons at multiple choice points. *Neural Dev.* 2008;3:34.

36. Renaud J, Kerjan G, Sumita I, et al. Plexin-A2 and its ligand, Sema6A, control nucleus-centrosome coupling in migrating granule cells. *Nature Neurosci.* 2008;11(4):440-449.

37. Matsuoka RL, Nguyen-Ba-Charvet KT, Parray A, Badea TC, Chedotal A, Kolodkin AL. Transmembrane semaphorin signalling controls laminar stratification in the mammalian retina. *Nature.* 2011;470(7333):259-263.

38. Saint-Geniez M, D'Amore PA. Development and pathology of the hyaloid, choroidal and retinal vasculature. *Int J Dev Biol.* 2004;48(8-9):1045-1058.

39. Lang RA, Bishop JM. Macrophages are required for cell death and tissue remodeling in the developing mouse eye. *Cell.* 1993;74(3):453-462.

40. Fruttiger M. Development of the retinal vasculature. *Angiogenesis.* 2007;10(2):77-88.

41. Campochiaro PA, Hackett SF. Ocular neovascu-

larization: a valuable model system. *Oncogene.* 2003;22(42):6537-6548.

42. Gavard J, Hou X, Qu Y, et al. A role for a CXCR2/ phosphatidylinositol 3-kinase gamma signaling axis in acute and chronic vascular permeability. *Mol Cell Biol.* 2009;29(9):2469-2480.

43. Scheppke L, Aguilar E, Gariano RF, et al. Retinal vascular permeability suppression by topical application of a novel VEGFR2/Src kinase inhibitor in mice and rabbits. *J Clin Invest.* 2008;118(6): 2337-2346.

44. Shojaei F, Wu X, Qu X, et al. G-CSF-initiated myeloid cell mobilization and angiogenesis mediate tumor refractoriness to anti-VEGF therapy in mouse models. *Proc Natl Acad Sci U S A.* 2009; 106(16):6742-6747.

45. Little GE, Lopez-Bendito G, Runker AE, et al. Specificity and plasticity of thalamocortical connections in Sema6A mutant mice. *PLoS Biol.* 2009;7(4):e98.

46. Klostermann A, Lutz B, Gertler F, Behl C. The orthologous human and murine semaphorin 6A-1 proteins (SEMA6A-1/Sema6A-1) bind to the enabled/vasodilator-stimulated phosphoprotein-like protein (EVL) via a novel carboxyl-terminal zyxin-like domain. *J Biol Chem.* 2000;275(50): 39647-39653.

47. Nogi T, Yasui N, Mihara E, et al. Structural basis for semaphorin signalling through the plexin receptor. *Nature.* 2010;467(7319):1123-1127.

48. Zhou Q, Gallagher R, Ufret-Vincenty R, Li X, Olson EN, Wang S. Regulation of angiogenesis and choroidal neovascularization by members of microRNA-23~27~24 clusters. *Proc Natl Acad Sci U S A.* 2011;108(20):8287-8292.

49. Urbich C, Kaluza D, Fromel T, et al. MicroRNA-27a/b controls endothelial cell repulsion and angiogenesis by targeting semaphorin 6A. *Blood.* 2011;119(6):1607-1616.

50. Gelfand MV, Hong S, Gu C. Guidance from above: common cues direct distinct signaling outcomes in vascular and neural patterning. *Trends Cell Biol.* 2009;19(3):99-110.